ISSN (Print) 1226-1750
ISSN (Online) 2233-6656
Journal of Magnetics 26(2), 175-181 (2021) https://doi.org/10.4283/JMAG.2021.26.2.175

Entropy Optimized Hydro-Magnetic Flow Darcy-Forchheimer Viscous Fluid

Ying-Qing Song[1], Sohail. A Khan[2]*, M. Ijaz Khan[3], M. Y. Malik[4], and Ali S. Alqahtani[4]

[1]*College of Science, Hunan City University, Yiyang 413000, P. R. China*
[2]*Department of Mathematics, Quaid-I-Azam University 45320, Islamabad 44000, Pakistan*
[3]*Department of Mathematics and Statistics, Riphah International University I-14, Islamabad 44000, Pakistan*
[4]*Department of Mathematics, College of Sciences, King Khalid University, Abha 61413, Saudi Arabia*

(Received 11 April 2021, Received in final form 22 June 2021, Accepted 23 June 2021)

Here hydromagnetic flow of an incompressible Dary-Forchheimer fluid over a curved stretching surface is addressed. Heat source/sink and dissipation effects are considered in heat equation. Entropy generation is discussed through thermodynamics law. Bejan number is calculated. The proposed system are modeled in curvilinear coordinates. Partial differential system are reduced to ordinary one through transformation. ND-solve method is implemented to solve the given system. Graphical outcomes of velocity, entropy rate, temperature and Bejan number against flow variables are discussed. Numerical outcomes of drag force against pertinent variables are examined through table. Higher Hartman number decreases velocity field. A reverse effect for velocity is observed through porosity and curvature variables. An improvement in temperature is seen for curvature variable. An augmentation in entropy rate is noted for Brinkman number.

Keywords : darcy-forchheimer flow, curved stretching surface, heat source/sink, viscous dissipation, entropy generation and bejan number

1. Introduction

Darcy's law discussed the flow of fluid falling a porous space. Henry Darcy gives concept of Darcy's law on basis of experimental result [1]. The situation of flow transport in porous medium is concern of modern progress in geophysical and engineering processes. These actions are experienced in demand like system of ground water, nuclear reactors cooling, cleaning vessels of gas, grain storage gas and many others. Hong *et al.* [2] reported the non-Darcian effect in convective flow towards nonuniform porous vertical plate. Hayat *et al.* [3] considered the cubic autocatalysis reaction in radiative Darcy-Forchheimer flow over nonlinear stretched surface. Ganesh *et al.* [4] scrutinized hydromagnetic Darcy-Forchheimer nanoliquid flow by a shrinking/stretching sheet with Ohmic dissipation. Influence of second order slip in Darcy-Forchheimer micropolar ferrofluid flow subject to stretchable surface is illustrated by Khan *et al.* [5]. Seth *et al.* [6] scrutinized entropy rate in Darcy-Forchheimer flow of CNTs over stretched sheet. Some pertinent analyses about Darcy-Forchheimer flow are constructed in Refs. [7-20].

It is known fact that entropy rate is directly proportional to the degraded energy in a thermodynamic system. Therefore significant amount of energy is reduced when entropy optimization occurs. This concept is significant in air conditioners heat pumps, heat engines and power plants. Entropy generation (EG) depends mainly on the following factors: heat transfer, chemical reactions, mass transfer, power transmission, viscosity losses and simultaneous effects of thermal and solutal transfer Initially Bejan [21, 22] discussed the entropy problems in convective flow. Irreversibility and melting heat analysis in dissipative flow Newtonian nanofluid towards a stretched surface is analyzed by Khan *et al.* [23]. Some investigation about irreversibility problem is highlighted in Refs. [24-35].

The main theme of this article is to analyze the irreversibility analysis in MHD flow of Newtonian fluid over a stretching surface. Heat expression is communicated through heat source/sink and dissipation. Physical feature of entropy generation through second law of thermodynamics. Both cases PST and PHF for heat transportation phenomena are discussed. Similarity trans-

*Corresponding author: Tel: +923450149450
Fax: +923450149450, e-mail: sohailahmadkhan93@gmail.com

formation is used to get ordinary equation. The given system is solved through ND-solve method. Prominent effect of flow variables on velocity profile, Bejan number, temperature and entropy generation are discussed. Computational outcomes of drag force for pertinent variables are scrutinized through table.

2. Statement

Here two-dimensional magnetohydrodynamic flow of Darcy-Forchheimer viscous fluid subject to curved surface is addressed. Heat source/sink and dissipation in heat equation is scrutinized. Physical feature of entropy rate is discussed through second law of thermodynamics. Bejan number is calculated. Consider $u = as$ stretching velocity with positive rate constant ($a > 0$). Magnetic force of constant strength (B_0) is applied in r-direction. Flow sketch is presented in Fig. 1.

The governing equations satisfy [1-5]:

$$\frac{\partial}{\partial r}\left((r+R)v\right)+R\frac{\partial u}{\partial s}=0, \tag{1}$$

$$\frac{\partial p}{\partial r}-\frac{\rho}{r+R}u^2=0, \tag{2}$$

$$\rho\left(v\frac{\partial u}{\partial r}+\frac{uR}{r+R}\frac{\partial u}{\partial s}+\frac{uv}{r+R}\right)=-\frac{R}{r+R}\frac{\partial p}{\partial s} +\mu\left(\frac{\partial^2 u}{\partial r^2}+\frac{1}{r+R}\frac{\partial u}{\partial r}-\frac{u}{(r+R)^2}\right)-\sigma B_0^2 u-\frac{\mu}{k^*}u-Fu^2 \tag{3}$$

$$\left.\begin{aligned} &v\frac{\partial T}{\partial r}+\frac{uR}{r+R}\frac{\partial T}{\partial s}=\frac{k}{(\rho c_p)}\left(\frac{1}{r+R}\frac{\partial T}{\partial r}+\frac{\partial^2 T}{\partial r^2}\right)\\ &+\frac{\mu_f}{(\rho c_p)}\left(\frac{\partial u}{\partial r}+\frac{u}{r+R}\right)^2+\frac{Q_0}{(\rho c_p)}(T-T_\infty)\end{aligned}\right\} \tag{4}$$

with boundary conditions [44-46]:

$$\left.\begin{aligned} &u=u_w=as,\quad v=0,\\ &\begin{cases} T=T_w \text{ for PST case}\\ -k\frac{\partial T}{\partial r}=D\left(\frac{s}{l}\right)^2 \text{ for PHF case}\end{cases}\quad \text{at } r=0\\ &u\to 0,\ \frac{\partial u}{\partial r}\to 0,\ T=T_\infty,\ \text{as}\quad r\to\infty.\end{aligned}\right\} \tag{5}$$

Considering the transformation

$$\left.\begin{aligned} &u=asf'(\eta),\ v=-\frac{R}{r+R}\sqrt{av_f}\,f(\eta), p=\rho_f a^2 s^2 P(\eta),\ \eta=\sqrt{\tfrac{a}{v}}r.\\ &\begin{cases}\theta(\eta)=\frac{T-T_\infty}{T_w-T_\infty}, \text{ for PST}\\ T-T_\infty=\frac{D}{k}\left(\frac{s}{l}\right)^2\sqrt{\tfrac{v}{a}}g(\eta), \text{ for PHF}\end{cases}\end{aligned}\right\} \tag{6}$$

One can write

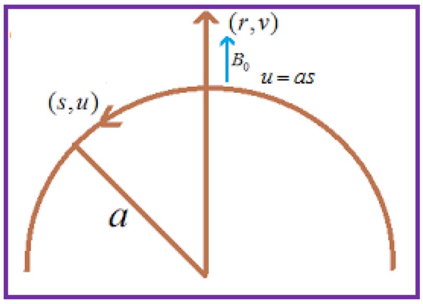

Fig. 1. (Color online) Flow sketch.

$$P'=\frac{f'^2}{(\eta+K)}, \tag{7}$$

$$\left.\begin{aligned}&\frac{2K}{(\eta+K)}P=f'''+\frac{1}{(\eta+K)}f''-\frac{K}{(\eta+K)}f'-\frac{K}{(\eta+K)}f'^2\\ &+\frac{K}{(\eta+K)}ff''+\frac{K}{(\eta+K)^2}ff',\ -\beta f'-Frf'^2-Mf'.\end{aligned}\right\} \tag{8}$$

$$\theta''+\frac{1}{(\eta+K)}\theta'+\frac{\Pr K}{(\eta+K)}f\theta'+Br\left(f''+\frac{1}{(\eta+K)}f'\right)^2 +\Pr Q\theta=0, \tag{9}$$

$$\left.\begin{aligned}&f(0)=0,\ f'(0)=1,\\ &\begin{cases}\theta(0)=1, \text{ for PST}\\ g'(0)=-1, \text{ for PHF}\end{cases}\end{aligned}\right\} \tag{10}$$

$$\left.\begin{aligned}&f'(\infty)=0,\ f''(\infty)=0,\\ &\begin{cases}\theta(\infty)=0, \text{ for PST}\\ g(\infty)=0, \text{ for PHF}\end{cases}\end{aligned}\right\}0 \tag{11}$$

Here dimensionless parameters are $K\left(=\sqrt{\tfrac{a}{v}}R\right)$, $\beta\left(=\tfrac{v}{ak^*}\right)$, $M\left(=\tfrac{\sigma B_0^2}{a\rho}\right)$, $Fr\left(=\tfrac{C_b}{\sqrt{k^*}}\right)$, $\Pr\left(=\tfrac{v}{\alpha}\right)$, $Q\left(=\tfrac{Q_0}{a(\rho c_p)}\right)$, $Ec\left(=\tfrac{a^2 s^2}{c_p(T_w-T_\infty)}\right)$ and $Br(=\Pr Ec)$.

By neglecting P from Eqs. (8) and (7), we have

$$\left.\begin{aligned}&f^{iv}+\tfrac{2}{(\eta+K)}f'''-\tfrac{1}{(\eta+K)^2}f''+\tfrac{1}{(\eta+K)^3}f'+\tfrac{K}{(\eta+K)}\left(ff'''-ff''\right)\\ &+\tfrac{K}{(\eta+K)^2}\left(ff''-f'^2\right)-\tfrac{K}{(\eta+K)^3}ff'-\beta\left(f''-\tfrac{1}{(\eta+K)}f''\right)\\ &-Fr\left(2ff''+\tfrac{1}{(\eta+K)}f'^2\right)-M\left(f''-\tfrac{1}{(\eta+K)}f'\right)\end{aligned}\right\} \tag{12}$$

3. Surface Drag Force

It is given by

$$C_{fs} = \frac{\tau_{rs}}{\rho (u_w)^2}, \tag{13}$$

shear stress τ_{rs} satisfy

$$\tau_{rs} = \mu_f \left(\frac{\partial u}{\partial r} + \frac{R}{r+R}\frac{\partial v}{\partial s} - \frac{u}{r+R} \right)\bigg|_{r=0} \tag{14}$$

or

$$C_{fs}\,\mathrm{Re}_s^{1/2} = f''(0) - \frac{f'(0)}{K} = f''(0) - \frac{1}{K}. \tag{15}$$

4. Entropy Modeling

It is expressed as

$$E_G = \frac{k}{T_\infty^2}\left(\frac{\partial T}{\partial r}\right)^2 + \frac{\mu_f}{T_\infty}\left(\frac{\partial u}{\partial r} + \frac{u}{r+R}\right)^2 + \frac{\mu}{k^* T_\infty}u^2, \tag{16}$$

one can have

$$S_G = \alpha_1 \theta'^2 + Br\left(f'' + \frac{1}{(\eta+K)}f'\right)^2 + MBrf'^2 + \beta Brf'^2. \tag{17}$$

Bejan number mathematically satisfy

$$Be = \frac{\alpha_1\theta'^2}{\alpha_1\theta'^2 + Br\left(f'' + \frac{1}{(\eta+K)}f'\right)^2 + \beta Brf'^2}. \tag{18}$$

Here dimensionless parameters are $\alpha_1\left(=\frac{\Delta T}{T_\infty} = \frac{T_w - T_\infty}{T_\infty}\right)$ and $S_G\left(=\frac{E_G T_\infty \nu}{ak(T_w - T_\infty)}\right)$.

5. Discussion

Influence of velocity, Bejan number, temperature and entropy rate versus various sundry parameters are examined. Computational outcomes of drag force are discussed through table.

5.1. Velocity

Influence of Hartman number on velocity is interpreted in Fig. 2. An intensification in Hartman number corresponds to rises resistive force. Therefore velocity is reduced. Fig. 3 drafted to show the influence of velocity against porosity variable. Higher porosity reduces the velocity profile ($f'(\eta)$). Effect of Forchheimer number on velocity is demonstrated in Fig. 4. Clearly one can found that velocity is declined through Forchheimer.

5.2. Temperature

Physical feature of Brinkman number on temperature ($\theta(\eta)$ and $g(\eta)$) for both PST and PHF cases is demonstrated in Figs. 5, 6. An amplification in Brinkman number improves the temperature for both PST and PHF cases. Figs. 7, 8 sketched to see the impact of curvature variable on temperature ($\theta(\eta)$ and $g(\eta)$). Clearly noted that higher curvature variable lead to augments temperature for both PST and PHF cases. Influence of heat generation variable on temperature for both PST and PHF is demonstrated in Figs. 9, 10. An intensification in heat generation variable corresponds to improve the temperature for both PST and PHF cases.

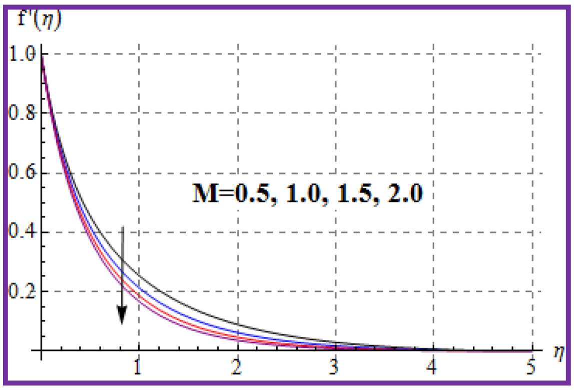

Fig. 2. (Color online) $f'(\eta)$ via M.

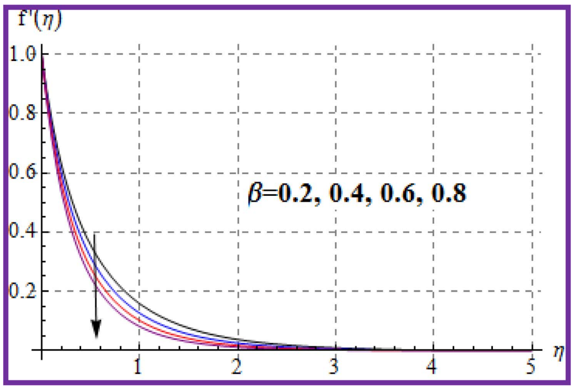

Fig. 3. (Color online) $f'(\eta)$ via β.

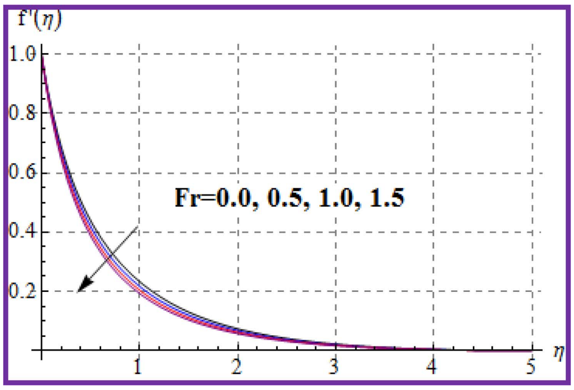

Fig. 4. (Color online) $f'(\eta)$ via Fr.

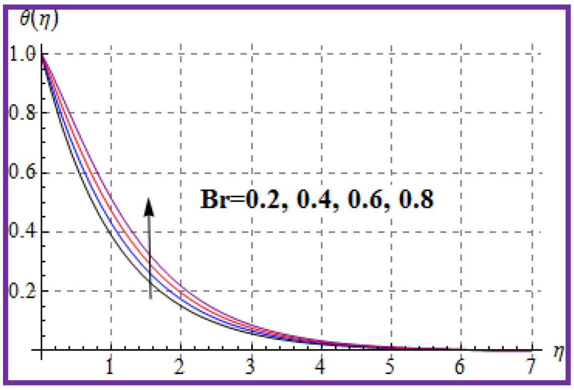

Fig. 5. (Color online) $g(\eta)$ via *Br*.

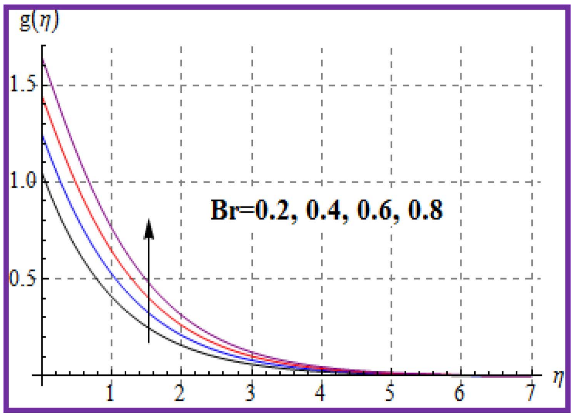

Fig. 6. (Color online) $g(\eta)$ via *Br*.

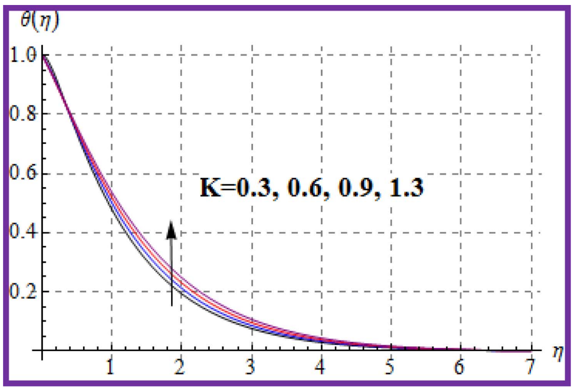

Fig. 7. (Color online) $\theta(\eta)$ via *K*.

5.3. Entropy rate and Bejan number

Influence of porosity variable on ($S_G(\eta)$) and (*Be*) is portrayed in Figs. 11, 12. An increment in porosity variable lead to rises both ($S_G(\eta)$) and (*Be*) for both PST and PHF cases. Physically higher (β) leads to augments resistance to the liquid flow and thus entropy boosted. Figs. 13, 14 sketch to show impact of ($S_G(\eta)$) and (*Be*) via curvature variable. An intensification in curvature variable has reverse effect on ($S_G(\eta)$) and (*Be*) for both PST and PHF cases. Performance of Brinkman number on ($S_G(\eta)$) and (*Be*) is illuminated in Figs. 15, 16. Higher approximation of (Br) rises the entropy rate for both PST and PHF cases. While opposite effect is observed for Bejan number.

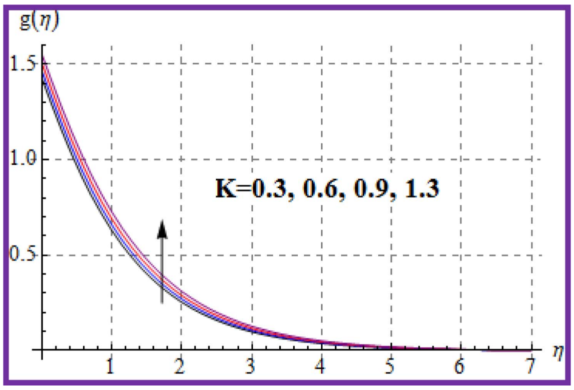

Fig. 8. (Color online) $g(\eta)$ via *K*.

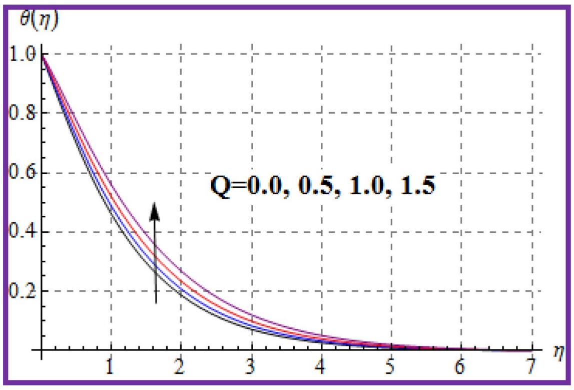

Fig. 9. (Color online) $\theta(\eta)$ via *Q*.

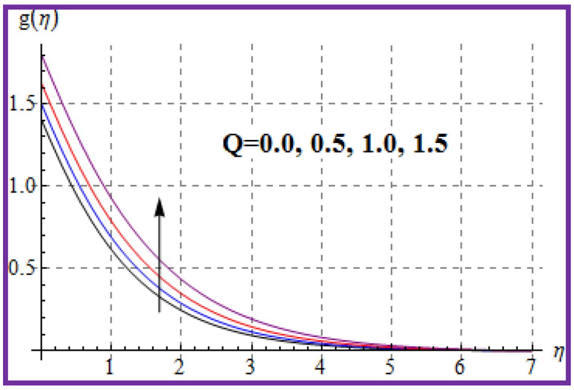

Fig. 10. (Color online) $g(\eta)$ via *Q*.

5.4. Skin friction coefficient

Physical description of drag force versus curvature variable and Hartman number is discussed in Table 1. An improvement in drag force is seen for Hartman number.

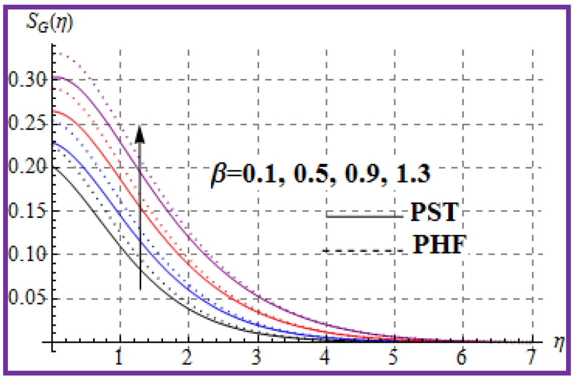

Fig. 11. (Color online) $S_G(\eta)$ via β.

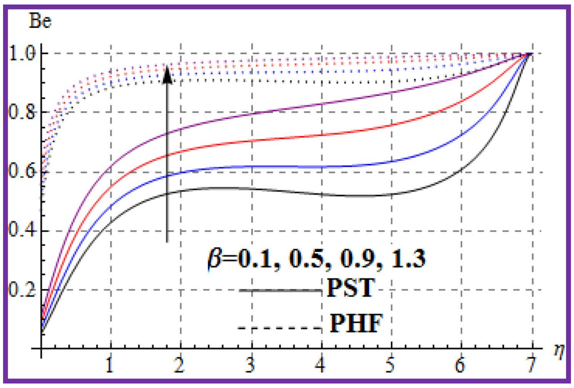

Fig. 12. (Color online) Be via β.

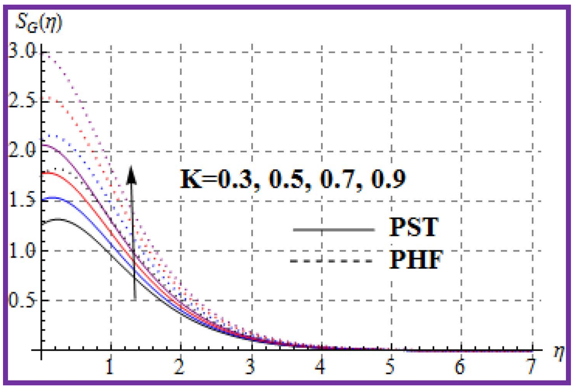

Fig. 13. (Color online) $S_G(\eta)$ via K.

Higher curvature variable leads to improve drag force ($C_{fs}\,\mathrm{Re}_s^{1/2}$).

6. Conclusions

The main observations are given below.

· A reverse effect for velocity field in observed via Forchheimer and Hartman numbers.

· As anticipated there is reduction in velocity for porosity variable.

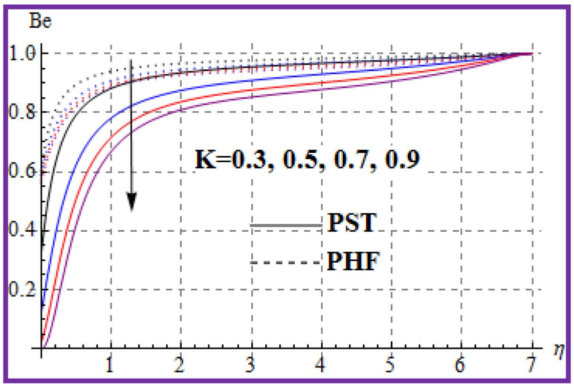

Fig. 14. (Color online) Be via K.

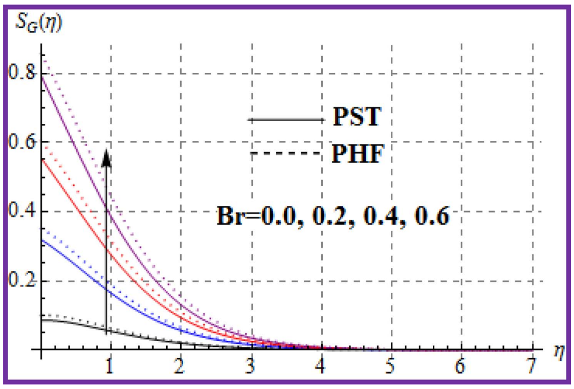

Fig. 15. (Color online) $S_G(\eta)$ via Br.

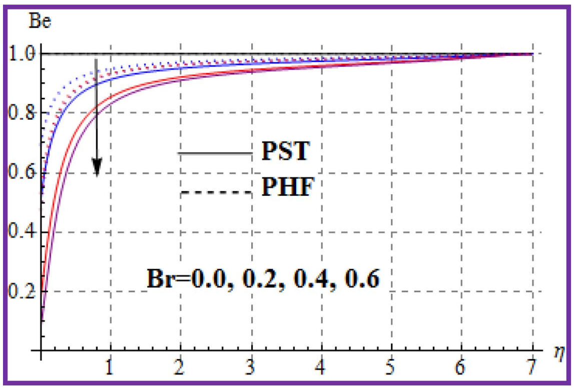

Fig. 16. (Color online) Be via Br.

Table 1. Skin friction values via flow parameters.

K	M	$C_{fs}\mathrm{Re}_s^{1/2}$
0.3	0.3	1.03654
0.6		0.894563
1.0		0.756321
0.5	1.0	2.23654
	2.0	2.56423
	3.0	2.76532

- Temperature and velocity enhancement is noted through curvature parameter.
- Temperature for heat generation/absorption variable and Brinkman number is augmented.
- Magnetic parameter leads to temperature distribution enhancement.
- An opposite scenario for curvature variable is noticed through Bejan number and entropy generation rate.
- An increment in entropy rate is observed for Brinkman number.
- An enhancement in Bejan number and entropy rate is observed via porosity parameter.
- Hartman number correspond to velocity gradient enhancement.
- Gradient of velocity has enhancing trend for curvature parameter.
- Nusselt number for curvature parameter is reduced.

Acknowledgment

The authors extend their appreciation to the Deanship of Scientific Research at King Khalid University, Abha 61413, Saudi Arabia for funding this work through research groups program under grant number R. G. P-1/96/42.

Nomenclature

u, v	velocity components
r, s	curvilinear coordinates
p	pressure
T	temperature
T_w	wall temperature
T_∞	ambient temperature
ρ	density
ν	kinematic viscosity
μ	dynamic viscosity
k^*	porous medium permeability
σ	electrical conductivity
F	non-uniform inertia coefficient
C_b	drag force
c_p	specific heat
k	thermal conductivity
D	constant
K	curvature parameter
β	porosity parameter
M	Hartman number
Fr	Forchheimer number
Pr	Prandtl number
Q	heat generation/absorption parameter
Ec	Eckert number
Br	Brinkman number
Cf_s	skin friction coefficient
τ_{rs}	shear stress
Nu_s	Nusselt number
q_w	heat flux
Re_s	local Reynold number
S_G	entropy generation rate
Be	Bejan number
α_1	temperature difference parameter

References

[1] P. Forchheimer, Wasserbewegung Durch Boden, Zeitschrift des Vereins Deutscher Ingenieure **45**, 1782 (1901).
[2] J. T. Hong, Y. Yamada, and C. L. Tien, J. Heat Trans. **109**, 356 (1987).
[3] T. Hayat, F. Shah, A. Alsaedi, and Z. Hussain, Resul. Phy. **7**, 2497 (2017).
[4] N. V. Ganesh, A. K. A. Hakeem, and B. Ganga, Ain. Sham. Eng. J. **9**, 939 (2018).
[5] M. I. Khan, F. Alzahrani, and A. Hobiny, J. Mater. Rese. Technol. **9**, 7335 (2020).
[6] G. S. Seth, R. Kumar, and A. Bhattacharyya, J. Mol. Liq. **268**, 637 (2018).
[7] T. Sajid, M. Sagheer, S. Hussain, and M. Bilal, AIP. Advan. **8**, 035102 (2018).
[8] M. Jawad, Z. Shah, S. Islam, E. Bonyah, and A. Z. Khan, J. Phys. Commun. **2**, 115014 (2018).
[9] A. Zaim, A. Aissa, F. Mebarek-Oudina, B. Mahanthesh, G. Lorenzini, and M. Sahnoun, Propu. Power Resea. **9**, 383 (2020).
[10] S. M. Abo-Dahab, M. A. Abdelhafez, F. Mebarek-Oudina, and S. M. Bilal, Indian. J. Phy. (2021).
[11] Marzougui, M. Bouabid, F. Mebarek-Oudina, N. Abu-Hamdeh, M. Magherbi, and K. Ramesh, Int. J. Numer. Methods Heat Fluid Flow. (2020).
[12] T. Hayat, S. Qayyum, A. Alsaedi, and B. Ahmad, Int. Comm. Heat Mass Tran. **111**, 104445 (2020).
[13] S. Z. Abbas, W. A. Khan, S. Kadry, M. I. Khan, M. Waqas, and M. I. Khan, Com. Meth. Prog. Biomed. **190**, 105363 (2020).
[14] S. A. Khan, T. Saeed, M. I. Khan, T. Hayat, M. I. Khan, and A. Alsaedi, Int. J. Hyd. En. **44**, 31579 (2019).
[15] D. Pal and H. Mondal, Int. Comm. Heat Mass Tran. **39**, 913 (2012).
[16] M. Jawad, Z. Shah, S. Islam, E. Bonyah, and A. Z. Khan, J. Phys. Commun. **2**, 115014 (2018).
[17] F. Mebarek-Oudina, N. K. Reddy, and M. Sankar, Lecture Notes in Mechanical Engineering. Springer, Singapore. (2021).
[18] M. I. Khan, M. Waqas, T. Hayat, and A. Alsaedi, J. Colloid Interface Sci. **498**, 85 (2017).
[19] D. Das, P. Biswal, M. Roy, and T. Basak, Int. J. Heat Mass Tran. **97**, 1044 (2016).

[20] M. K.Nayak, S. Shaw, M. I. Khan, V. S. Pandey, and M. Nazeer, J. Mater. Rese. Technol. **9**, 7387 (2020).
[21] A. Bejan, CRC Press: New York, NY, USA, 1996.
[22] A. Bejan, Energy Int. J. **5**, 721 (1980).
[23] S. A.Khan, T. Hayat, A. Alsaedi, and B. Ahmad, Renew. Sustain. Energy Rev. **140** (2021).
[24] T. Tayebi, H. F. Öztop, and A. J. Chamkha, Ther. Sci. Eng. Prog. 100605 (2020).
[25] F. Mebarek-Oudina, R. Fares, A. Aissa, R. W. Lewis, and N. Abu-Hamdeh, Int. Communi. Heat Mass Trans. **125**, 105279 (2021).
[26] Z. Zhang, C. Lou, Z. Li, and Y. Long, J. Quantit. Spectro. Radiat. Tran. **253**, 107175 (2020).
[27] T. Hayat, S. A. Khan, M. I. Khan, and A. Alsaedi, Com. Meth. Prog. Biom. **177**, 279 (2019).
[28] M. I. Khan, S. Ullah, T. Hayat, M. I. Khan, and A. Alsaedi, J. Mol. Liq. **260**, 279 (2018).
[29] E. O. Fatunmbi and A. Adeniyan, Res. Eng. **6**, 100142 (2020).
[30] F. Mebarek-Oudina, A. Aissa, B. Mahanthesh, and H. F. Öztop, Int. Communi. Heat Mass Trans. 117, 104737 (2020).
[31] T. Hayat, M. W. Ahmad, M. I. Khan, and A. Alsaedi, Com. Meth. Prog. Biom. **184**, 105105 (2020).
[32] I. Khan, W. A. Khan, M. Qasim, I. Afridi, and S. O. Alharbi, Entropy **21**, 74 (2019).
[33] K. S. A. Kalbani, M. M. Rahman, and M. Z. Saghir, Int. J. Thermofluid. **5-6**, 100031 (2020).
[34] T. Hayat, S. A. Khan, M. I. Khan, and A. Alsaedi, Phys. Scr. **94**, 085001 (2019).
[35] M. I. Khan and F. Alzahrani, J. Theoret Computat. Chemis. **34** (2020).